A GEO-ELECTRICAL RESISTIVITY CONCEPTUAL MODEL UPDATE FOR THE MENENGAI GEOTHERMAL SYSTEM

D. S. Saitet[1], M. O. K'Orowe[2] and N. O. Mariita[1]
[1] Kenya Electricity Generating Company, Olkaria
[2]Jomo Kenyatta University of Agriculture and Technology Nairobi, Kenya
E-mail: modondi@yahoo.com

Abstract
A geo-electrical conceptual model for the Menengai geothermal prospect is built using magnetotellurics data both of low and high amplitude collected over time. The data is corrected for static shift by use of transient electromagnetic data collected at the same data stations. Data collected previously in the same area using these techniques is also incorporated into the working data base. The entire data set is jointly inverted and cross sections taken along four profiles cutting across the caldera and intersecting major structures in the area. An interpretation of these results show the existence of geothermal indicators within the caldera bounds with a general north-eastern to south-western trend and is significantly shallower towards the east

Key words: Geothermal, Menengai, resistivity, MT, TEM, AMT

1.0 Introduction

Previous studies carried out at Menengai did not adequately cover the area within the caldera. The major reasons were that the caldera floor was perceived as a volcanic risk as well as the challenges posed by its rugged terrain. More recent surveys involved data collection in part of the caldera but there were still large data gaps for a conclusive delineation of geothermal resources in the prospect. There was therefore need for collection of infill data to reasonably understand the resistivity structure beneath the prospect area.

The techniques used in prior studies were to a large extent direct current resistivity methods (DC) with some enhancement using magnetotellurics methods (MT) in the later studies. The DC methods could not penetrate to sufficient depths especially due to the limitation on the length of the loop and presence of resistive lava piles near the surface. MT soundings on the other hand suffer static shift problems (Jones, 1988). A method of correction proposed by Sternberg *et al.,* 1988 and Pullerin and Hohman, 1990 has been widely adopted to correct these shifts by applying time domain electromagnetic soundings at the same location as those of MT. This method is applied for correction in this work.

Magnetotellurics methods are based on induced electromagnetic fields whose sources are outside the earth and therefore are not affected by terrain and electrode polarization, as is the case for DC methods.
Through their use of a wide range of frequencies they are capable of probing the subsurface from shallow to much deeper levels.

The use of Audio Magnetotellurics (AMT) alongside ordinary MT techniques enhances the integrity of near surface resistivity structure. Thirty three (33) new AMT/MT data were collected to infill data gaps and the resultant dataset was jointly inverted with TEM and MT data available for the study area.
This resulted in a more closely spaced resistivity data set hence a clearer view of the components of the system and their characteristics may be better understood.

1.1 Geological and Tectonic Setting

Menengai is a relatively seismically active area located in the region where the failed Kavirondo rift branch joins the main Kenyan rift. Two rift floor tectonovolcanic axes (Molo and Solai) terminate at the Menengai complex (KenGen, 2004). Menengai volcano is estimated to be of Pliocene age (McCall, 1967) and consists of a large collapsed caldera covering an approximate area of about 70km2. The caldera floor is composed of panteliric trachytes (KenGen, 2004) with a ring of Menengai tuff covering most of the area from the west side extending through the south to the north east side. Shield trachytes are observed further south. The caldera is superimposed on an area dominated by pyroclastics extending to the Olrongai and Olobanita volcanic centres. A structural map of the

study area (Figure 1) shows the location of the caldera in relation to the two TVAs and the rift fault. Figure 2 shows a geological map of the Menengai region and the surrounding areas.

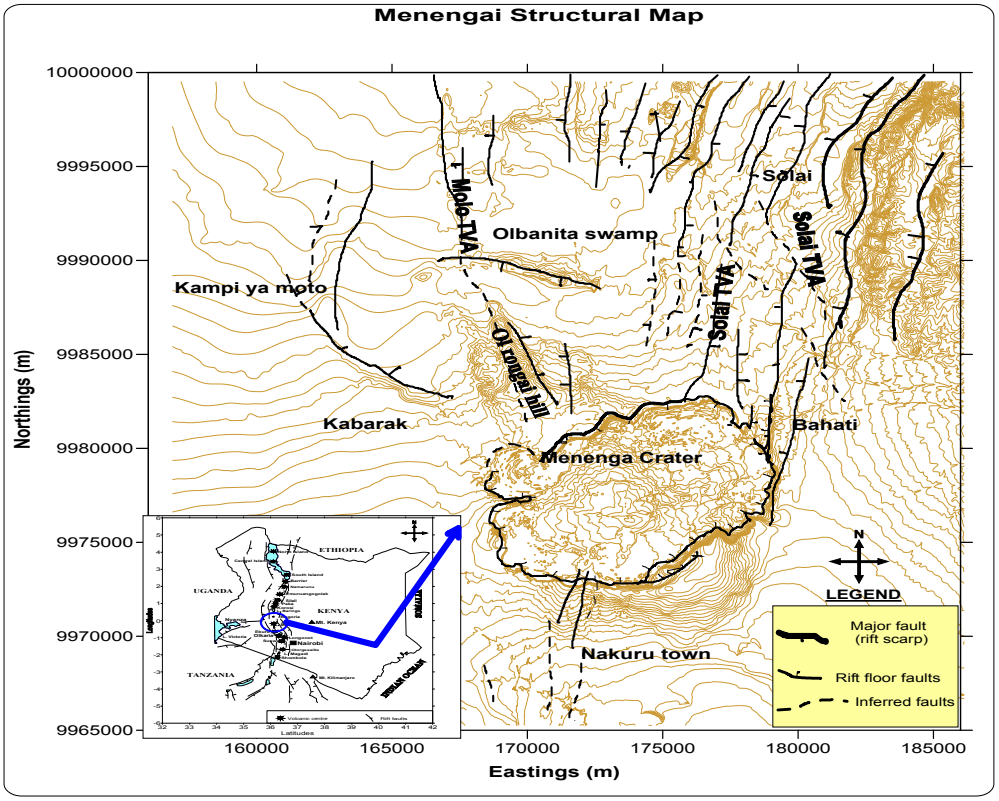

Figure 1: A structural map of Menengai showing its location at the intersection of two major tectono-volcanic axes and elevation contours. Inset is the map of Kenya showing the location of Menengai

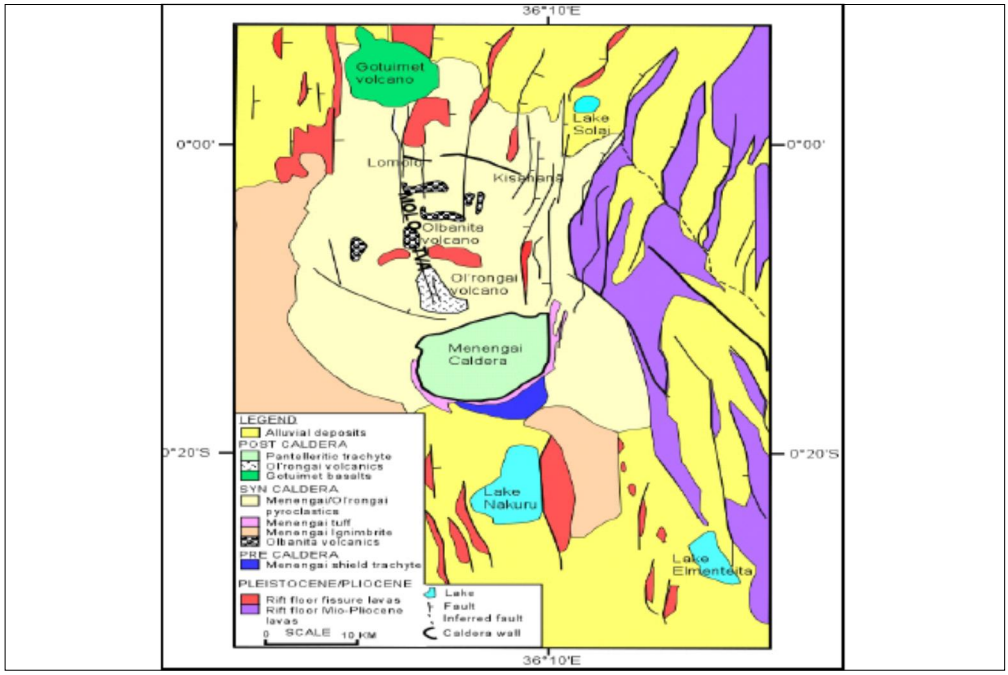

Figure 2: Geological map of Menengai and its Environs (KenGen, 2004)

1.2 Theoretical Concept

The Magnetotelluric (MT) and Audiomagnetotelluric (AMT) methods are electromagnetic (EM) sounding techniques that use surface measurements of the natural electric (E) and magnetic (B) fields to infer the subsurface electrical resisstivity distribution. AMT and MT methods are essentially the same, differing only in the frequency range captured. The lower the frequency, such as the case of MT the deeper the penetration. The AMT technique acquires data in the frequency range of about 1 KHz to 10 KHz, which is the range of human hearing hence the 'audio' prefix. The MT technique is sensitive to frequencies in the range 10-4 to 104 Hz. These frequency bands provide information used to delineate structures at depth. The techniques rely on detection of small potential differences generated by electromagnetic waves propagated from the ionosphere (Ward and Wannamaker, 1983). AMT/ MT data at various frequencies provide a means to distinguish spatial variations in apparent resistivity of the medium. The apparent resistivity is calculated from the ratio of E and B magnitudes using Cagniard equation of 1995;

$$\rho_a = \frac{0.2}{f}\left|\frac{E}{B}\right|^2 \quad (1)$$

where ρ^a is apparent resistivity, f, is frequency, E, is electric field and B is magnetic field.

The skin depth, Z, to which MT field penetrates is a function of frequency and resistivity and is given by Faufman and Keller equation of 1988 as:

$$Z=\left(\frac{2}{\omega\mu\sigma}\right)^{2}=503\sqrt{\frac{\rho}{f}} \quad (2)$$

where ρ, is resistivity of substrate.

The apparent resistivity for decreasing frequency thus provides resistivity information at progressively increasing depths.

Near surface, the resistivity inhomogeinities distort electric field due to discontinuities across resistivity boundaries. This is known as static shift. This in effect shifts the MT sounding curve (of apparent resistivity versus period) by some scale factor. Since magnetic field is relatively unaffected, by static shift, a controlled source magnetic field sounding, such as transient electromagnetic sounding (TEM) can be used to correct for static shift. The MT curve is shifted vertically so that the high frequency part of the MT curve coincides with TEM curve. The low frequency MT curve then gives an undistorted view of the deep resistivity section. In the central loop transient electromagnetic method (TEM), a steady current is transmitted in a transmitter wire loop laid on the ground at the area to be studied. The current is allowed to flow for a sufficiently long time to allow turn-on transients in the ground to dissipate (Figure 3). The steady current is abruptly terminated in a controlled manner. At the instance of transmitter turn –off, eddy currents reproduce the static magnetic field in the transmitter loop but then decay rapidly. The decaying primary magnetic field induces eddy currents immediately below the transmitter loop. As the initial near-surface eddy currents decay, its distribution in the ground in turn induces a secondary magnetic field that also decays with time. The process continues over time with ever weakening secondary magnetic field currents at increasing depth.

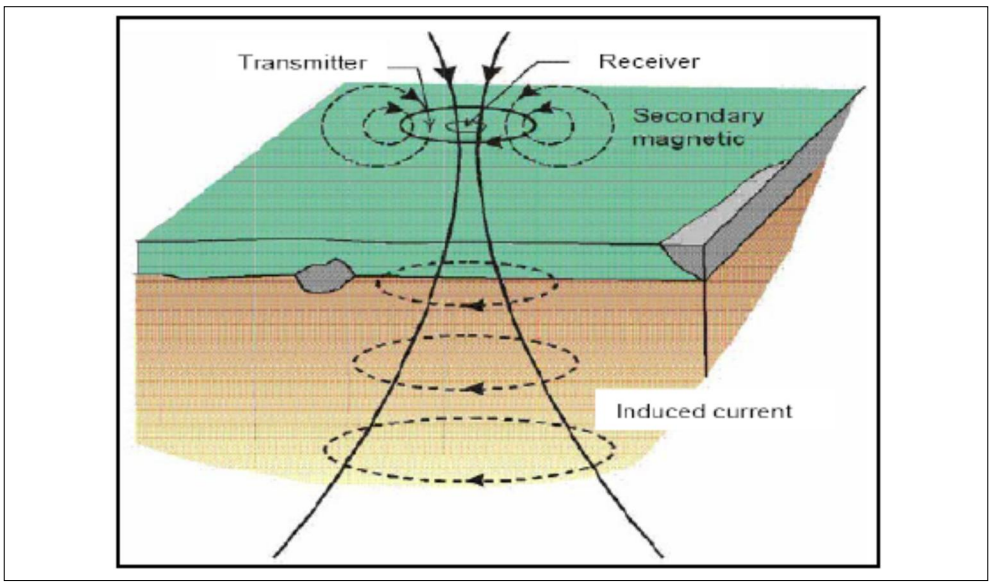

Figure 3: Transient current flow in ground

The magnitude and rate of decay of the secondary magnetic field is monitored by measuring the voltage induced in a receiver coil, placed at the centre of the transmitter loop, as a function of time after transmitter current is turned off. This is interpreted in terms of subsurface resistivity structure (A'mason, 1989).

The apparent resistivity ρ_a, in terms of induced voltage at later times after the source current is turned off is given as:

$$\rho_a = \frac{\mu_o}{4\pi}\left[\frac{2\mu_o A_r n_r A_s n_s}{5t^{3/2}V(t,r)}\right]^{2/3}$$

where: t= time elapsed after the transmitter current is turned off,

A_r = cross-sectional area of the receiver coil (m^2)

n_r = number of windings in the receiver coil

μ_o = magnetic permeability in vacuum

A_s = cross-sectional area of transmitter loop

n_s =number of windings in transmitter loop

V (t, r) = measured voltage.

2.0 Methodology

In this study TEM soundings were carried out at the same stations with MT so that static shift problem with MT could be resolved using TEM results. In a bid to obtain a clearer resolution of near surface structure AMT soundings were also collected at the same stations as TEM and MT. These data were used to validate TEM data for shallow depths as well as provide a continuation of deep MT results. The stations are shown in figure 6.

The equipment used is an MT/AMT unit (MT-5A).To ensures good contact with the ground; the ports were soaked with clean water that had been salted with common salt. The three magnetic electrodes were buried at about 1 foot depth and oriented as shown in the figure 4. The four telluric ports were also shallowly buried with a solution of Bentonite.A car battery was used to power the system. The unit collected data continuosly for at least 18 hours at each station for MT and 1 hour for AMT.

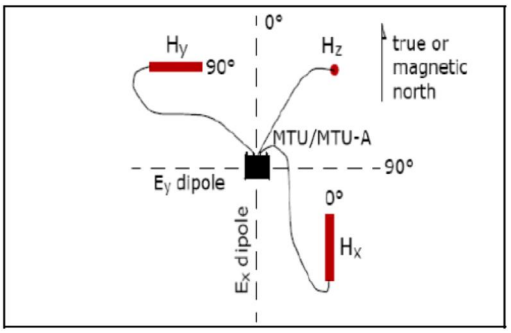

Figure 4: A field array for a 5 channel MT data acquisition system (Phoenix Geophysics ltd.)

In the transient electromagnetic (TEM) method an electrical current is injected into the ground and its decay and the magnetic field created are measured in order to infer the resistance of subsurface formations. The TEM method can effectively resolve earth resistivity structure down to 2 km.

For TEM soundings an arrangement shown in Figure 5 was applied where a half-duty square wave current was transmitted into a 300 m x 300 m transmitter wire loop at frequencies of 16 Hz and 4 Hz. The transmitter was synchronized with the data processor so that at current turn-offs, the processor coil retrieved data from the receiver coil.

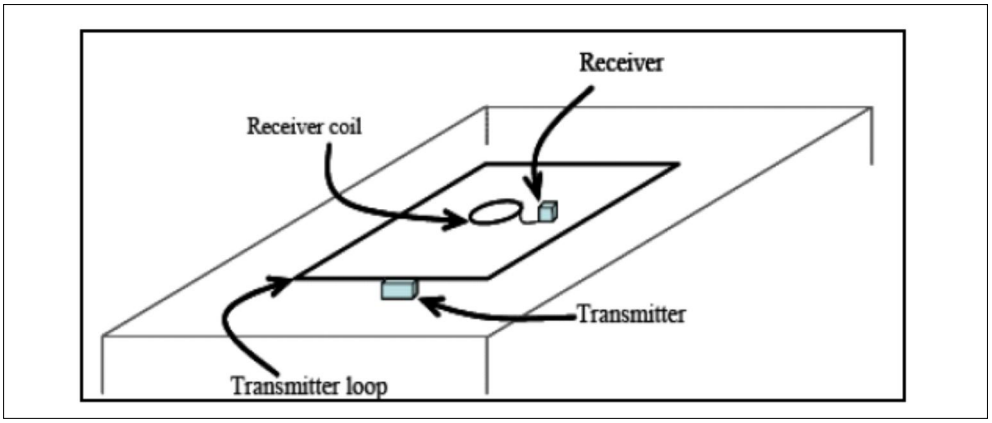

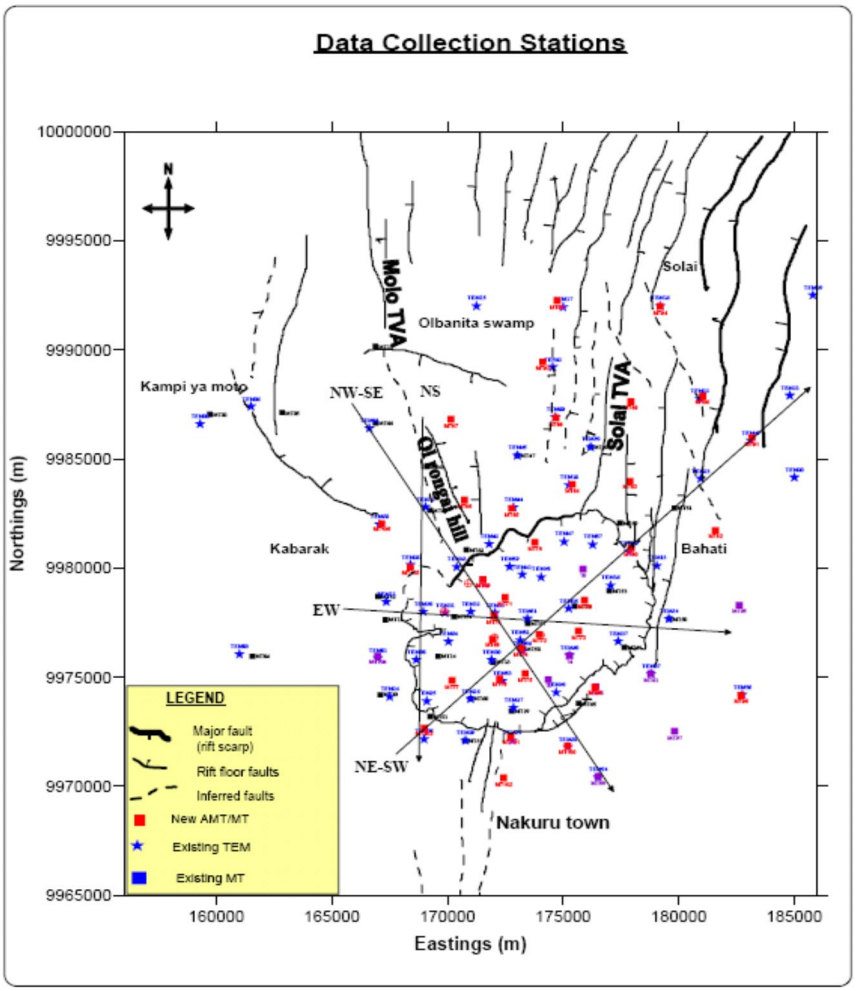

3.0 Data Analysis

Time-series data were downloaded using the SSMT2000 software from the MT unit and were processed using MTeditor (Phoenix Geophysics-Canada). The SSMT2000 was used to configure A/MT instrumentation and parameters. The MTeditor accepts MT plots output by SSMT2000, mergees the crosspowers and displays MT parameters graphically. It also enables elimination of crosspowers from the calculations and hence the possibility of editing out poor data.

The primary objective of editing is to create a smooth resistivity curve by eliminating those cross-powers that have been moved too far from the mean by noise and related effects.

The resulting data were then converted into the standard format accepted by the 'WinGlink'integrated interpretation software. A well established method for static shift correction of MT data is the use of TEM (Stenberg *et al,* 1988; Pullerin and Hohmann, 1990).

The imported 1-D model is used to calculate a forward MT response. The observed apparent resistivity curve can then be shifted along the resistivity axis to coincide with the values suggested by the TEM response.

Joint inversion of A/MT and TEM data is performed to deduce 1-D smooth models of the subsurface resistivity structure as well as resisstivity isomaps at different depths, elevations and frequencies. Layered resistivity models are then calculated from the smooth models. Three cross sections (Figures 7, 8 and 9) were taken to delineate the depth and geometry of observed resistivity results which are presented in the form of contour models.

4.0 Results and Dicussions

To better appreciate the resistivity variations with depth across the study area, 2-D cross-sections namely, East-West (E-W), North-South (N-S) and North East-South West (NE-SW) are shown in figures 7, 8 and 9

E-W Profile

In this profile (Figure 7), regions of high resistivity (>120 ohm-m) are observed at the ends of the profile. A low resistivity anomaly (<20 ohm-m) cuts across the central region at 500msl. A more conductive cap is noticed along this profile. There are two possible reservoirs observed on the profile. The area underlying TEM 35 and TEM 37 (between 7,000 m and 11,000 m from the origin of profile). Due to scarce data to the eastern end of the caldera to conclusively draw any conclusions. This anomalous region is separated from the second one by a deep conductive segment that originates from the eastern caldera wall. This conductive zone may be the area where meteoric waters mix with hot geothermal water. Ionised cooler water flows deeper and the buoyant hot water rises.

The second reservoir occurs to the West and intrudes the Western caldera wall extending to the central caldera area. The resistive body (>120 ohm-m) extends from sea level to depth with a shallow conductive cap at about 500m depth. This may be attributed to the hot reservoir with a conductive cap of thermal altered material.

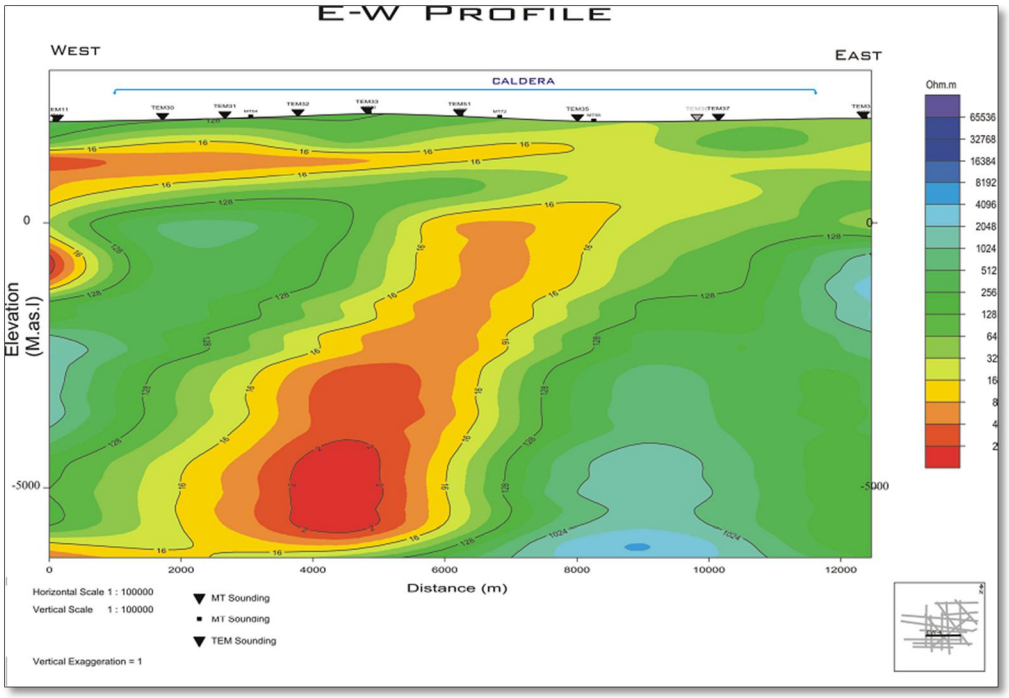

Figure 7: East- West Profile

N-S Profile

The N-S profile that cuts across the western sector of the caldera (Figure 8) shows two high resistivity regimes. The first of these anomalies occurs directly below Olrongai Hill and is characterized by a resistive body at about 500msl that is enclosed by two conductive regimes. The trend of the outlined body aligns with the Molo TVA. This regime is separated from the second one by a narrow vertical feature with low resistivity that coincides with the Northern caldera wall and runs deep.

In the second anomaly, a thick conductive segment about 500 m thick, separates surface resistive rocks with a successively increasing rresistive section that runs dep reaching some 6000 m depth from the surface. This anomaly shows classical geothermal reservoir characteristics. Meteoric recharge is interpreted as entering the system through the fractured caldera wall to the South and the waters are heated as they percolate through hot rock and mix with heated geothermal water. A similar scenario is observed at the boundary of the caldera.

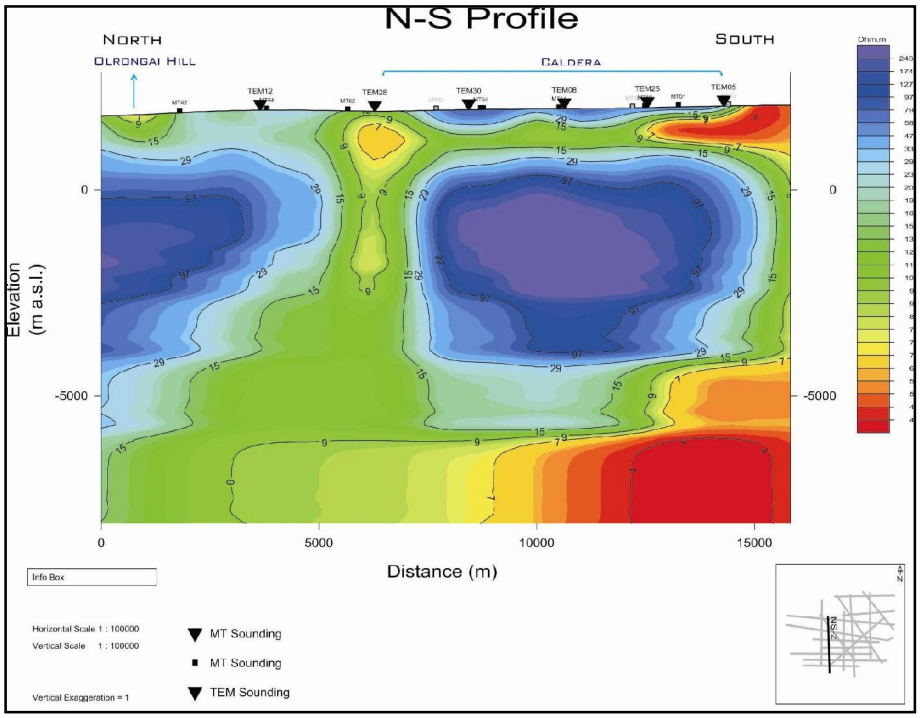

Figure 8: North - South Profile

NE-SW Profile

In the profile, Figure 9, a resistive intrusive material coincides with the Solai TVA to the North East with formations extending upwards from about 500m depth to the surface. This structure delineates the extent of the interpreted geothermal system to be confined within the bounds of the caldera. An anomaly located between 2000m and 9000m along the profile may be associated with a reservoir. It is observed to diminish both in size and resistivity signature to the North-East. This profile shows that the system observed in the Eastern part of the caldera may be viewed as being independent to that located at the centre of the caldera that extends both westwards and southwards.

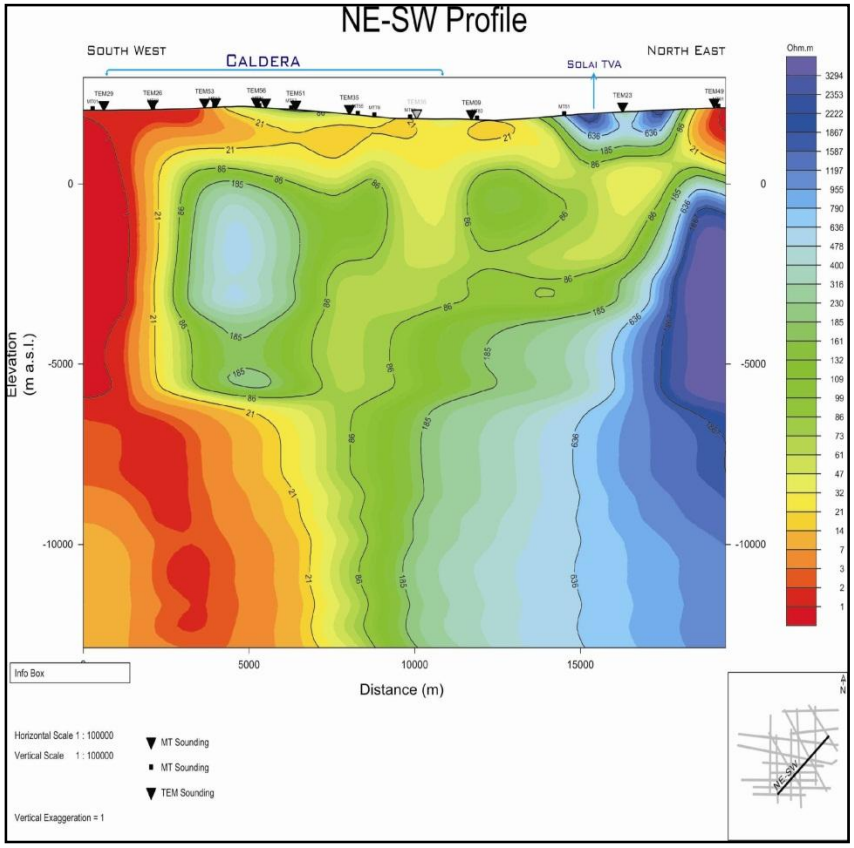

Figure 9: North East- South West Profile

5.0 Discussion

The analysis of resistivity 2-D cross sections across the caldera presented in Figures 7, 8 and 9 shows a body with reservoir characteristics that lie directly below the caldera but which trends in a northeastern-southwestern fashion that gets significantly shallow towards the east. A similar structure is observed below Olrongai hill (northwest) but appearing to have been separated from the earlier resource by major north-south fractures coinciding with the western caldera wall. These structures extend to depth and possibly control deep vertical permeability in this area. The results are then interpreted alongside findings form a wide array of previous work in gravity (Simiyu and Keller, 1997, Mariita, 2003) seismic (Simiyu and Keller, 1997) and a comprehensive multidisciplinary study by KenGen (KenGen, 2004) which formed good constraints in developing the conceptual model of the system.

Fresh meteoric water percolates into the system from precipitation at the flanks of the rift through numerous fractures and gets heated at depth by heated water and rock material becoming buoyant and rising along permeable zones of the reservoir.

Two conceptual models are constructed along the East West profile (Figure 10) and the North East-South West profile (Figure 11).

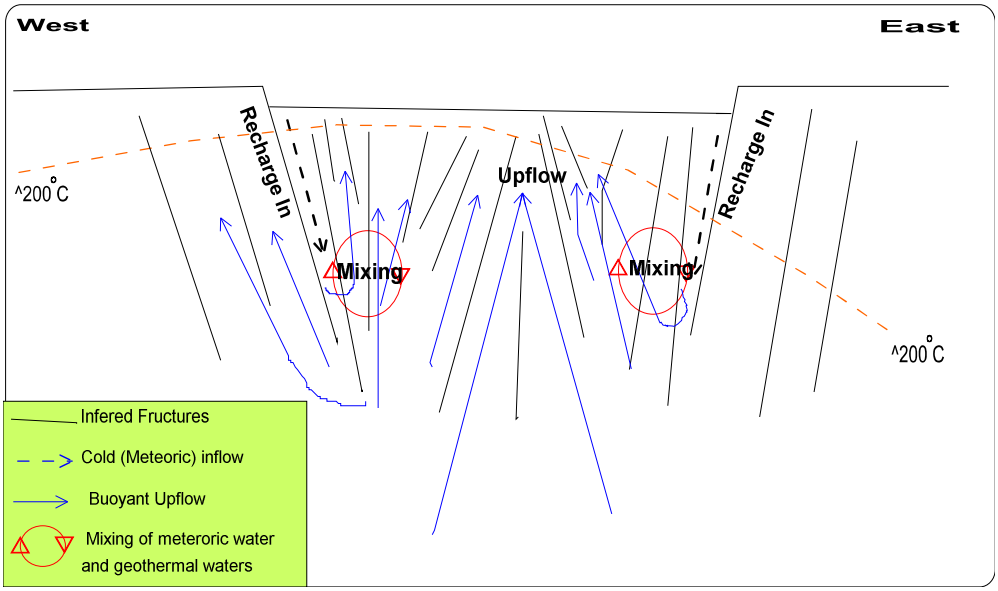

Figure 10: *A conceptual model along the E-W profile across the caldera showing up flow zones to the west and at the central part of the caldera.*

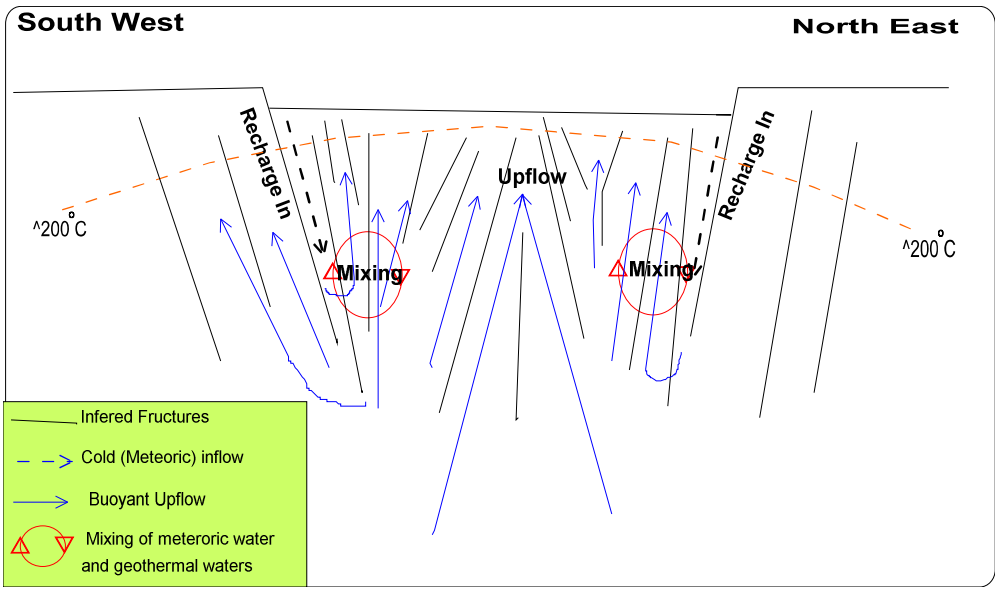

Figure. 11: Conceptual model of the prospect along the SW-NE profile. Three up flow zones are shown; to the SW, at the central caldera region and to the NE.

6.0 Conclusion

Exploitable geothermal resources exist at Menangai. The resources are to a large extent found directly beneath the caldera floor with little extension outside the caldera. The heat source is shallower towards the east.

The two TVAs intersecting at the complex control most permeability in the area. A possible location of further resources appears to be below the Olrongai hill to the west with the Molo TVA and the north-south trending faults providing a structural discontinuity separates this system from the other.

The Menengai geothermal system recharges from precipitation at the flanks of the rift with possible up flow zones located at the central, south western and north eastern caldera sectors.

References

A'rmason K., (1989). Central loop transient electromagnetic sounding over horizontal layered earth. Orkustofnun, Reykjavic, report OS-89032/JHD-06, pp. 129

Jones A.G., (1988). Static shift of magnetotelluric data and its removal in a sedimentary basin environment. *Geophysics*, 53-7, pp. 967-978.

KenGen (2004), Menengai Volcano: Investigations for its geothermal potential-a geothermal resource assessment project.

Mariita N. O., (2003): An integrated geophysical study of the northern Kenya rift crustal structure: implications for geothermal energy prospecting for Menengai area. *A PhD dissertation, University of Texas at El Paso, USA*.

McCall G. J. H, (1967): Geology of the Nakuru-Thomson's fall-Lake Hannington Area, Degree Sheet No. 35 SW and 43 NW Quarter.

Pullerin L., Hohmann and G. W., (1990). Transient Electromagnetic Inversion: A remedy for Magnetotelluric static shifts: *Geophysics,* 55, pp. 1242-1250.

Simiyu S. M., and Keller G. R., (1997), Integrated geophysical analysis of the East African Plateau from gravity anomalies and recent seismic studies. *Tectonophysics,* 278, pp. 291-314.

Sternberg B. K., Washbourne J. C., Pullerin, L., (1988), Correction for the static shift in Magnetotellurics using Transient Electromagnetic soundings. *Geophysics,* 53, pp. 1459-1468.

Ward S. H, and Wannamaker P. E. (1983). The MT/AMT electromagnetic method in geothermal exploration, UNU-GTP, Iceland, report 5, pp. 107.